Original Article

Trends in Hearing
2017, Vol. 21: 1–12

DOI: 10.1177/2331216517690108
journals.sagepub.com/home/tia
SAGE

Evaluating Multipulse Integration as a Neural-Health Correlate in Human Cochlear-Implant Users: Relationship to Psychometric Functions for Detection

Ning Zhou[1] and Lixue Dong[1]

Abstract

In electrical hearing, multipulse integration (MPI) describes the rate at which detection threshold decreases with increasing stimulation rate in a fixed-duration pulse train. In human subjects, MPI has been shown to be dependent on the psychophysically estimated spread of neural excitation at a high stimulation rate, with broader spread predicting greater integration. The first aim of the present study was to replicate this finding using alternative methods for measuring MPI and spread of neural excitation. The second aim was to test the hypothesis that MPI is related to the slope of the psychometric function for detection. Specifically, a steep *d'* versus stimulus level function would predict shallow MPI since the amount of current reduction necessary to compensate for an increase in stimulation rate to maintain threshold would be small. The MPI function was measured by obtaining adaptive detection thresholds at 160 and 640 pulses per second. Spread of neural excitation was measured by forward-masked psychophysical tuning curves. All psychophysical testing was performed in a monopolar stimulation mode (MP 1 + 2). Results showed that MPI was correlated with the slopes of the tuning curves, with broader tuning predicting steeper MPI, confirming the earlier finding. However, there was no relationship between MPI and the slopes of the psychometric functions. These results suggest that a broad stimulation of the cochlea facilitates MPI. MPI however is not related to the estimated neural excitation growth with current level near the behavioral threshold, at least in monopolar stimulation.

Keywords

multipulse integration, psychometric functions for detection, cochlear implants, psychophysical tuning curves

Date received: 16 September 2016; revised: 21 December 2016; accepted: 23 December 2016

Introduction

In electrical hearing with cochlear implants, detection thresholds often decrease with increasing stimulation rate for a fixed-duration pulse train (Kreft, Donaldson, & Nelson, 2004; McKay & McDermott, 1998; Zhou, Xu, & Pfingst, 2012). The rate of threshold decrease with increasing stimulation rate has been referred to as multipulse integration (MPI; Zhou, Kraft, Colesa, & Pfingst, 2015; Zhou & Pfingst, 2014). In implanted guinea pigs, it has been shown that MPI was dependent on the density of spiral ganglion cells (SGNs) near the stimulation site (Kang et al., 2010; Pfingst et al., 2011; Zhou et al., 2015). This relationship was the strongest for stimulation rates below 1,000 pulses per second (pps). In the implanted guinea pigs, the tested electrodes, which were in the apical end of the electrode array, filled much of the space in the scala tympani. Therefore, in those animal models, the distance between the electrodes and the target neurons was quite constant. With relatively constant electrode-neuron distance, the correlation between MPI and SGN density can be interpreted as the dependence of MPI on the number of SGNs near the stimulation site.

There are a few plausible mechanisms underlying the relationship between MPI and the number of SGNs. The rate of threshold decrease with increasing stimulation rate should correspond to the increase of neural activity

[1]Department of Communication Sciences and Disorders, East Carolina University, Greenville, NC, USA

Corresponding author:
Ning Zhou, 3310Y Health Sciences Building, Department of Communication Sciences and Disorders, East Carolina University, Greenville, NC, 27834, USA.
Email: zhoun@ecu.edu

in the temporal integration window as rate increases at a fixed current level. A larger ratio of neural activity increase with the increase of rate at a fixed current level would correspond to a greater improvement in threshold, that is, steeper MPI. The increase of neural activity would then depend on the extent to which single auditory fibers would increase their discharge rate to respond to the increase of stimulus power, or the extent to which an increasing number of neurons would engage to respond to the stimulus as rate increases. The excitability of single fibers with increasing rate would further depend on the temporal characteristics of the excited neurons, specifically their refractory, subthreshold accommodation, and adaptation time constants (e.g., Eggermont, 1985; Javel & Shepherd, 2000; Javel & Viemeister, 2000; McKay, Chandan, Akhoun, Siciliano, & Kluk, 2013; Miller, Woo, Abbas, Hu, & Robinson, 2011; Parkins, 1989; Smith & Brachman, 1982). The faster the fibers recover from prior stimulation, the steeper the integration (Zhou & Pfingst, 2016a). Alternatively, an increase in neural activity can be achieved by activating more neurons. The correlation between MPI and neural density in guinea pigs (e.g., Kang et al., 2010; Zhou et al., 2015) is consistent with this hypothesis. It was proposed that the neurons at the center of the current field are more likely to respond to stimulation when the stimulus is of low rate. Nonetheless, as rate increases, the neurons at the more peripheral locations of the current field would respond to stimulation when the excitability of the neurons at the center of the current field is reduced as a result of interpulse interactions, producing a spatial spread of neural excitation pattern and increased neural activity with the increase of stimulation rate. The number of neurons available for further recruitment as rate increases is perhaps smaller in guinea pigs in poorer neural condition than in those that are healthier.

In human subjects with cochlear implants, the scenario is more complex, for the number of excitable neurons is dependent on not only local neural density but also electrode-neuron distances (e.g., Long et al., 2014, 2015). Assuming equal neural survival conditions, the number of neurons available for excitation would be greater in the case of a far electrode, which produces a wide current field, compared with a close electrode scenario. It follows that the number of neurons available for further recruitment would be greater in a wider current field, when excitability of the neurons in the center of the current field is reduced by interpulse interaction with the increase of stimulation rate. Psychophysical results in humans indeed showed that steeper MPI slopes were associated with broader forward-masking patterns measured at a high stimulation rate (Zhou & Pfingst, 2016b). These results are consistent with the idea that the lowered threshold with an increase in stimulation rate is a result of activating more neurons rather than driving a fixed number of neurons to a higher spiking rate. Certainly, a broad masking pattern does not always suggest distant stimulation. Interaction between channels can be a result of a substantial loss of nerve fibers such that regions distant to the electrode must be stimulated to achieve the desired loudness. The stimulation sites tested in Zhou and Pfingst (2016b) were then further estimated for their electrode-neuron distances using CT-scanned distance measurements reported by Long et al. (2014, 2015) in subjects implanted with the same device types (CI24RE) as those tested in Zhou and Pfingst (2016b). Results showed that the stimulation sites with steep integration and broad masking patterns were typically those in the middle of the electrode array and were estimated to have a position far from the targeted neurons (Zhou & Pfingst, 2016b). There were a few exceptions where the broad masking patterns were not associated with steep MPIs. These stimulation sites were located at the very basal end of the electrode array where sizable nerve loss was suspected because those are the locations where neural degeneration typically first occurs. It was speculated that excitation was required to spread to achieve threshold, but the number of excited neurons was not necessarily large; therefore; the measured integration was poor (shallow MPI). There was only one case observed in Zhou and Pfingst (2016b), where the stimulation site produced a narrow forward-masking pattern as well as a relatively steep MPI slope, which would suggest a good neural survival region receiving narrow stimulation. This pattern however was rarely observed. The existing data suggest that, in human subjects, MPI was similarly dependent on the number of neurons involved in the integration process as was demonstrated in previous guinea pig studies. However, the required number of neurons for integration to occur is often only achieved by distant stimulation.

An alternative mechanism that could account for the variations in the MPI slopes is not related to neural density or neural excitability per se but is related to the slope of the psychometric function for detection (PFD). If *d'* grows slowly with the increase of current level, to maintain a given performance (threshold in case of MPI), the current reduction needed to compensate for an increase in rate would be large (Figure 1, left panel). On the contrary, if *d'* grows more steeply, as is shown on the right panel in Figure 1, the current reduction needed would be smaller to maintain a given performance. The idea is that a shallow MPI slope does not necessarily suggest that a change in stimulus produces little change in the neural representation of the stimulus but merely indicates a smaller current adjustment is needed to compensate for such change in the stimulus to maintain threshold. This is assuming that sensitivity to the signal (*d'*) reflects at least to some extent what occurs at the physiological level.

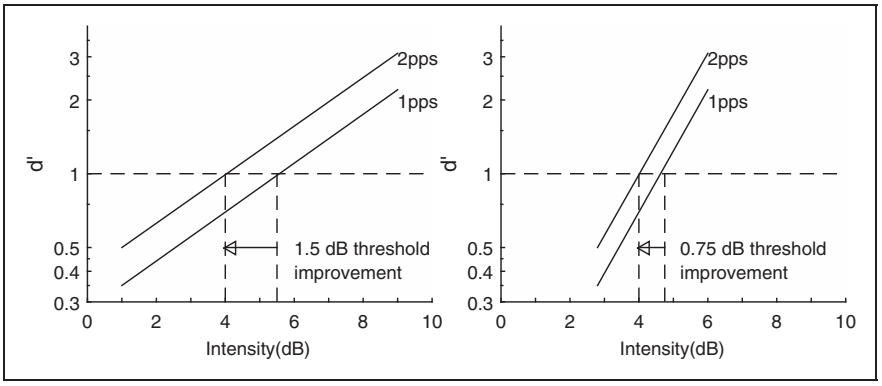

Figure 1. Psychometric functions for detection. Examples of shallow-sloped psychometric functions (left panel) and steep-sloped functions (right panel) and the relationship of the slopes of these functions to threshold improvement with increasing stimulation rate.

The objective of the current study was twofold. The first aim was to replicate the results from Zhou and Pfingst (2016b) using alternative psychophysical methods. In Zhou and Pfingst (2016b), the spatial selectivity of neural excitation was measured using a forward-masking paradigm, where the position of the probe was fixed and the spatial separation between the probe and the masker was varied. The slope of spatial decay of forward masking was used to estimate spread of neural excitation at the probe site. The maskers were loudness balanced. The caveat with loudness balancing the maskers was that a masker site in a relatively poor condition would require a higher absolute current level to achieve the designated loudness, but the high absolute current level would produce a greater amount of masking relative to the maskers of lower current levels (Cosentino, Deeks, & Carlyon, 2015). There was also an issue related to the robustness of thresholds estimated by a method of adjustment (MOA). In the current study, we therefore used more robust adaptive thresholds and an alternative measure for spatial selectivity, that is, the psychophysical tuning curves (PTCs), to confirm the relationship between MPI and estimated spread of neural excitation. The interpretation of PTCs can also be complicated by the difficulty of equating probe levels across sites and ears, as well as the difficulty of interpreting the meaning of masking levels at probe thresholds. Nonetheless, if the relationship between MPI and spatial spread holds across multiple measures, it would provide converging evidence for the robustness of the conclusion. The second aim of the current study was to explicitly test the alternative explanation for differences in MPI, namely that, MPI is related to the steepness of PFD.

The relationship between MPI and the psychophysically estimated neural function furthers our understanding of how the spatial neural activation pattern might interact with neural temporal response characteristics. This possible interaction might change our clinical thinking that spectral resolution in electrical hearing might be optimized independent of temporal resolution or vice versa.

Materials and Method

Subjects

Six subjects with Cochlear Nucleus® devices participated in the study. One of the bilateral implanted subjects was tested in both ears, resulting in a total N of 7 (see Table 1). For each ear, two stimulation sites were evaluated in the following psychophysical procedures. In the psychophysical testing, the subjects used a laboratory-owned Freedom processor. The stimuli were delivered in a monopolar stimulation (MP $1+2$) mode using MATLAB programs that connected with the NIC II research interface. All subjects provided written informed consent to participate in the following experiments. The use of human subjects in this study was approved by the East Carolina University Institutional Review Board.

Measuring Multipulse Integration

The stimuli for MPI were 250-ms biphasic trains with a phase duration of either 75 μs or 100 μs and an interphase interval of 8 μs. Detection thresholds were measured at two stimulation sites in each ear at two stimulation rates (160 pps and 640 pps). Thresholds were first estimated using MOA, where the subjects were asked to adjust the current level on their own to find the level at which the stimulus was just audible. The current level could be adjusted in step sizes of 25, 5, and 1 clinical level unit (CLU). The thresholds were then measured using a three-interval forced-choice paradigm (3IFC), where the signal occurred in one of the three intervals chosen at random. The subject was instructed

Table 1. Subject Demographics.

Subject	Ear	Gender	Age (years)	CI use (years)	Duration of deafness (years)	Implant type	Etiology
S1	Left	Male	76.21	13.08	0.6	CI24R (CS)	Hereditary
S1	Right	Male	76.21	7.1	6.0	CI24RE (CA)	Hereditary
S2	Right	Female	49.41	2.9	41.5	CI24RE (CA)	Nerve damage
S4	Left	Female	56.22	3.8	0.4	CI24RE (CS)	Hereditary
S6	Right	Female	83.64	3.4	65.2	CI24RE (CS)	Hereditary
S7	Right	Female	69.83	4.6	27.9	CI24RE (CS)	Nerve damage
S10	Right	Female	65.10	2.4	12.4	CI24RE (CS)	Hereditary

to choose the interval that contained the signal. The signal level started at 20 CLU above the MOA threshold and adapted following a 2-down 1-up criterion with a step size of 10 CLU for the first reversal, 5 CLU for the second, 2 CLU for the third, and 1 CLU for the remaining seven reversals. The average of the levels at the last six reversal points was taken as the threshold. For each stimulation site, MPI was quantified as the threshold decrease in dB per doubling of the stimulation rate.

Measuring PTCs

Next, the stimulation sites measured for MPIs were further evaluated for spatial tuning. The forward-masked PTCs were measured using biphasic pulse trains with a phase duration of 25 μs and an interphase interval of 8 μs. The forward masker was 300 ms long, followed by a 10-ms gap, and then the 20-ms probe. The maskers were placed on the three stimulation sites apical to the probe, on the same site as the probe, and three stimulation sites basal to the probe, when spatially possible. All seven maskers and the probe signal used a 900-pps stimulation rate. The unmasked probe threshold was first estimated using MOA and then measured using 3IFC following a similar procedure described earlier. When measuring the PTC, the level of the probe signal was set at 2 dB above its unmasked threshold and the level of the spatially varying maskers was adapted until the masker could just mask the probe. Using 3IFC, one of the three intervals chosen at random contained the masker-probe pair, where the masker was presented forward in time, followed by the gap and then the probe, whereas the other two intervals contained just the masker. The subjects were instructed to choose the interval that contained the sound with a *chirp* ending. The level of each masker started at 20% of its dynamic range and was adapted using a 1-down 2-up rule. The level adapted with a step size of 10 CLU for the first reversal, 5 CLU for the second, 2 CLU for the third, and 1 CLU for the remaining ten reversals. The level at which the masker could just mask the probe was determined for each masker-probe separation by taking the average of the masker levels at the last six reversal points. The procedure was repeated twice per stimulation site. The between-contact linear spacing in the recent Nucleus contour arrays (e.g., CI24RE) is not uniform and is narrower toward the apical end. The design was to maintain a uniform angular spacing between electrodes because the contour array is expected to be closer to the modiolus toward the more apical end. Forward masking was first fit against the actual probe-masker distance in mm and then against the probe-masker separation in terms of number of electrodes. The PTC slopes were calculated for the apical and basal sides of each function. Subjects were made aware of the temporal structure of the signal, that is, the masker-probe pair, and were asked to report when the chirp was not detectable, but the stimulus in one of the three intervals was longer than the others. This confusion would occur when the site's temporal resolution was not high enough to detect the gap between the masker and the probe (Neff, 1986). Once confusion occurred, and probe was confused as the continuation of the masker, particularly for on-site maskers, more repetitions were obtained to ensure the validity of the data.

Measuring Psychometric Functions for Detection

Psychometric functions for detection, that is, *d'* versus stimulus level, were obtained for the same stimuli that were used for measuring MPI, that is, 250-ms trains at 160 and 640 pps. For each ear, four PFDs were measured (2 Rates × 2 Sites). Each psychometric function was measured using the method of constant stimuli, in a two-interval forced-choice paradigm (2IFC). The adaptive thresholds obtained for MPI were used for estimating the level range of the constant stimuli that would produce performance ranging from 50% (chance) to 100%. The step size of the level increment and level range were estimated and modified, if necessary, for each stimulus and each site. The interval between adjacent levels was

typically 5 CLU. A step size of 3 CLU or smaller was used when the estimated level range was small. Using 2IFC, the signal was presented randomly in one of the two intervals. The signal level, which was predetermined, descended and ascended in an alternating fashion. Subjects were instructed to choose the interval with the signal. The test was administrated in blocks of 20 trials with each trial containing a descending and an ascending run. Percent correct scores as a function of current level were determined for each block. Three to six blocks were tested, corresponding to 120 to 240 presentations for each current level. The average percent correct score was then transformed to a *d'* unit, a measure for sensitivity, for each current level tested, assuming unbiased responses (Macmillan & Creelman, 2005). The slope of the psychometric function was derived by performing a linear fit for performance in log *d'* versus stimulus level in dB re 1mA.

Results

The raw MPI data are shown in Figure 2. Thresholds measured at the two rates are shown for each stimulation site and ear. It is apparent that the rate at which the threshold decreased with increasing stimulation rate (MPI slope) was quite variable across stimulation sites. The MPI slope was related to the absolute threshold level at the low stimulation rate. Using MPI as the dependent variable, the absolute threshold level as covariate, and subject as a random factor, the results of a univariate general linear model indicated that the absolute threshold level at 160 pps predicted the between-site variance in the MPI slopes, $F(1, 6) = 17.12$, $p = .006$, with higher threshold predicting steeper MPI. Threshold level at 640 pps did not have a relationship with MPI, $F(1, 6) = 0.851$, $p = .392$.

The forward-masked PTCs are shown in Figure 3. Missing data were sometimes due to the probe location being close to the apical or basal end of the array (e.g., S4L\E21) or masker level exceeding the site's maximum comfort level (C level) before the masker could mask the probe (e.g., S2R\E5). The tuning curves were often irregularly shaped and in rare cases nonmonotonic. The PTC slopes, fit based on probe-masker separation in number of electrodes, did not show a significant difference between the apical and basal sides of the functions, $t(13) = -1.6943$, $p = .114$. With the probe-masker

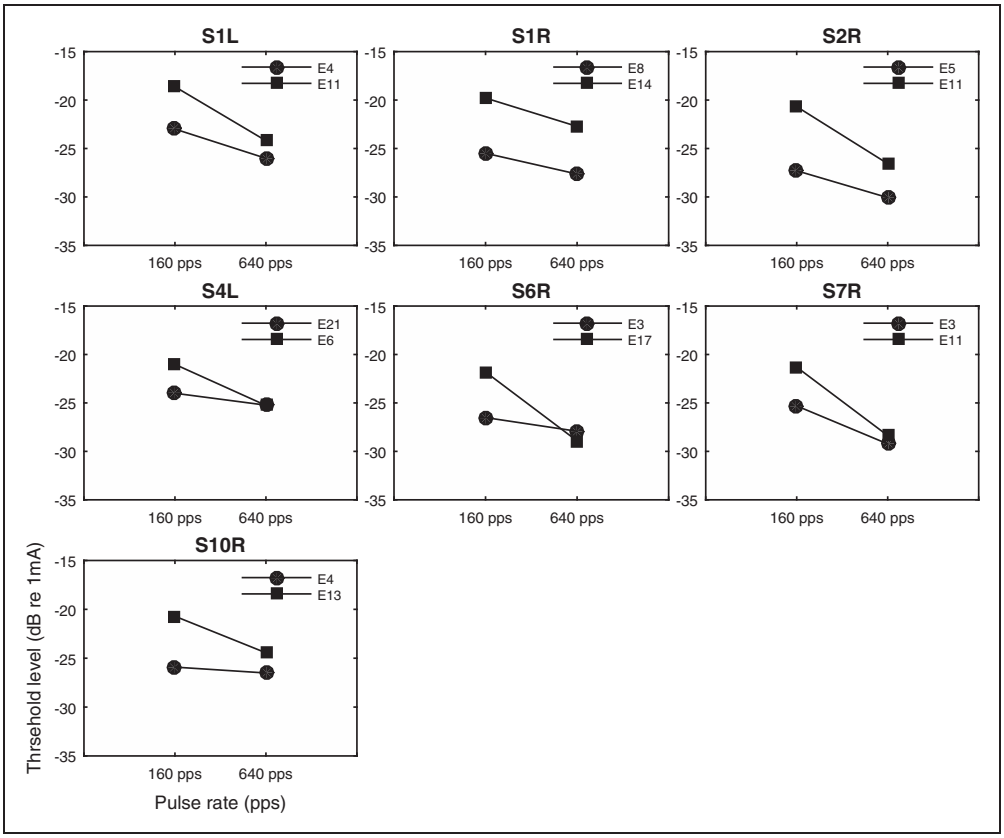

Figure 2. Absolute detection thresholds as a function of pulse rate (multipulse integrations). Each panel shows data from one ear. Detection thresholds are plotted as a function of stimulation rate. Symbols represent stimulation sites.

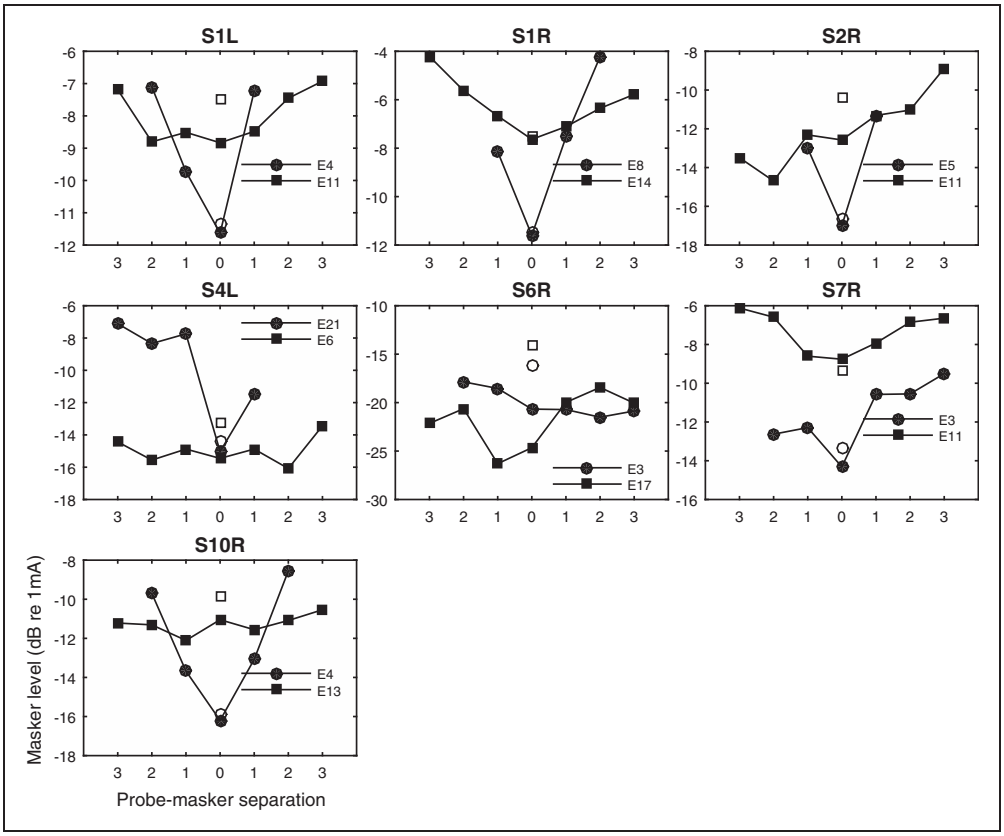

Figure 3. Forward-masked psychophysical tuning curves. The open symbols show unmasked probe thresholds. The filled symbols show masker levels required to just mask the probe set at 2 dB about its unmasked threshold against the spatial separation between the masker and probe. *X*-axis shows probe-masker separation in number of electrodes. Numbers left to 0 on the *x*-axis indicate maskers basal to the probe.

separation quantified in actual distance (mm), the slopes were significantly steeper on the apical sides than on the basal sides, $t(13) = -2.21$, $p = .045$. Since the uniform angular spacing between electrodes is only assumed, and the difference between the apical and basal PTC slopes fit based on actual mm spacing was significant although small, the slopes fit for the two sides of the function were considered separately in the following analysis.

The relationship between the slopes of the PTCs (in dB/mm) and MPIs is shown in Figure 4. Both sources of variance, that is, the between-site and between-ear variances in MPI were examined in a univariate general linear model. Results showed that the apical PTC slopes accounted for the between-site variance in the MPI slopes, $F(1, 6) = 12.51$, $p = .012$, but did not account for the between-ear variance in the MPI slopes, $F(6, 6) = 0.715$, $p = .653$. The basal PTC slopes similarly accounted for the between-site variance in the MPI slopes, $F(1, 6) = 7.327$, $p = .035$, but did not account for the between-ear variance in the MPI slopes, $F(6, 6) = 0.793$, $p = .606$. That is, within ears, the stimulation sites measured with broader tuning tended to be those that demonstrated steeper MPIs. In Figure 4, data were collapsed across stimulation sites and ears and then fit with linear lines for an easy visual inspection of data. The *R*-squared values shown in Figure 4 were adjusted for including both sources of variance. Since stimulation sites with higher absolute threshold levels at 160 pps were associated with steeper MPI, and those sites also tended to have broader tuning, the absolute threshold levels at 160 pps were also correlated with the sharpness of tuning, with higher thresholds predicting broader tuning—Apical: $r = -.757$, $p = .002$; Basal: $r = -.661$; $p = .01$.

Figure 5 shows PFD for the two stimuli (160 pps and 640 pps) measured at the two sites in each ear. The steepness of the psychometric functions was not related to the absolute current level at threshold. This was true for both the 160 pps, $r = .085$, $p = .77$, and 640 pps stimuli, $r = .069$, $p = .81$.

The relationships between the slopes of the psychometric functions and those of the MPI functions are shown in Figure 6. The slopes of the psychometric functions for the 160 pps stimulus did not correlate with those of MPI, $r = .2$, $p = .49$, nor did the slopes of the

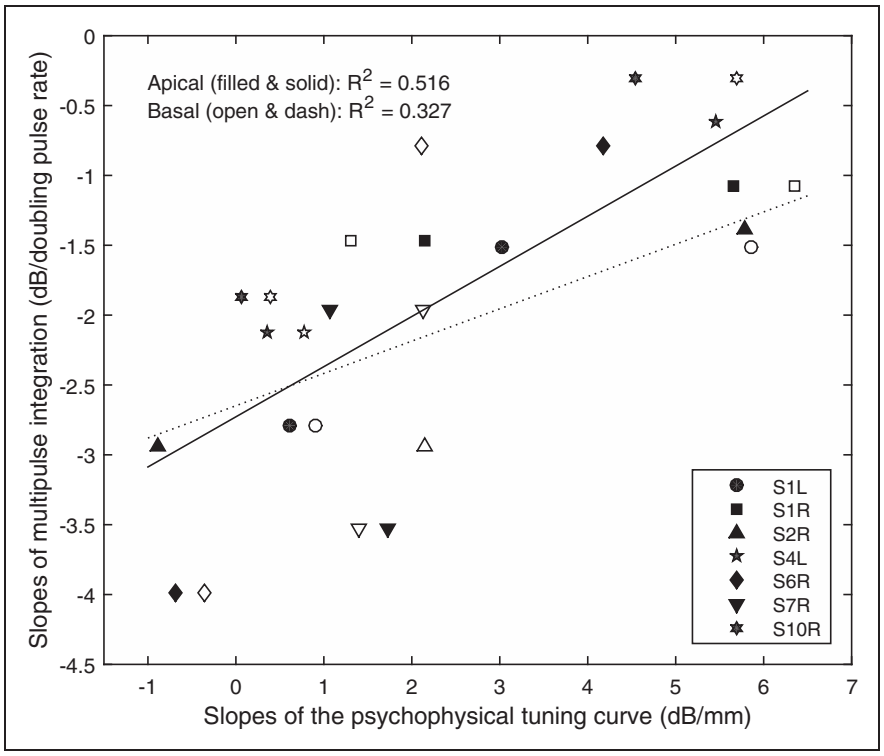

Figure 4. Scatter plot of the slopes of the multipulse integration functions against the apical (filled symbols) and basal (open symbols) slopes of the tuning curves. Stimulation sites and ears are collapsed in the plot. The line represents linear fit to the data. The *R*-squared values were corrected for examining two sources of variances in the general linear models.

psychometric functions for the 640 pps stimulus, $r = -.21$, $p = .48$, or the slopes averaged across rates, $r = .045$, $p = .88$. Consistent with the results of the Pearson's correlations, univariate general linear models also indicated that slopes of the psychometric functions for neither stimulus explained the between-site or between-ear variance in MPI.

Comparing slopes of the psychometric functions for the two stimuli of different rates, a repeated-measures *t* test revealed that the psychometric functions for the 160 pps stimulus were significantly steeper than those for the 640 pps stimulus, $t(13) = 2.8$, $p = .014$.

Discussion

The present study aimed to replicate a previous finding that the slopes of threshold decrease as a function of stimulation rate (MPI) correlate with a behavioral measure of spatial selectivity of neural excitation at a relatively high rate in human subjects with cochlear implants (Zhou & Pfingst, 2016b). Adaptive thresholds were used to quantify MPI and PTCs as a behavioral method to estimate the spread of neural excitation. Results confirmed the earlier finding that the MPI slopes were predicted by spread of neural excitation at 900 pps, with broader excitation predicting steeper MPI. The second aim of the study was to investigate an alternative theory that relates the steepness of MPI function to the slope of the PFD. Results showed that the MPI slopes were not related to the slopes of the PFD for either stimulus (160 pps and 640 pps). If we assume that the slope of the psychometric function correlates with the steepness of neural excitation growth with current level, there is no strong evidence to suggest that shallow MPIs were due to steep growth of neural excitation near threshold, at least in MP stimulation.

Relationship Between MPI and Tuning

The rationale for investigating MPI in human cochlear-implant subjects came from previous studies that found an association between the various cochlear health variables and the ear's ability to integrate electrical pulses in implanted guinea pigs (Kang et al., 2010; Pfingst et al., 2011; Zhou et al., 2015). One correlation that is particularly relevant to human subjects with cochlear implants is that the steepness of MPI is predicted by the density of SGNs near the stimulation site. There are several theories that offer plausible explanations for the variation in MPI, relating MPI directly to the quantity of the excitable auditory neurons, and indirect factors that might covary with neural density such as neural health

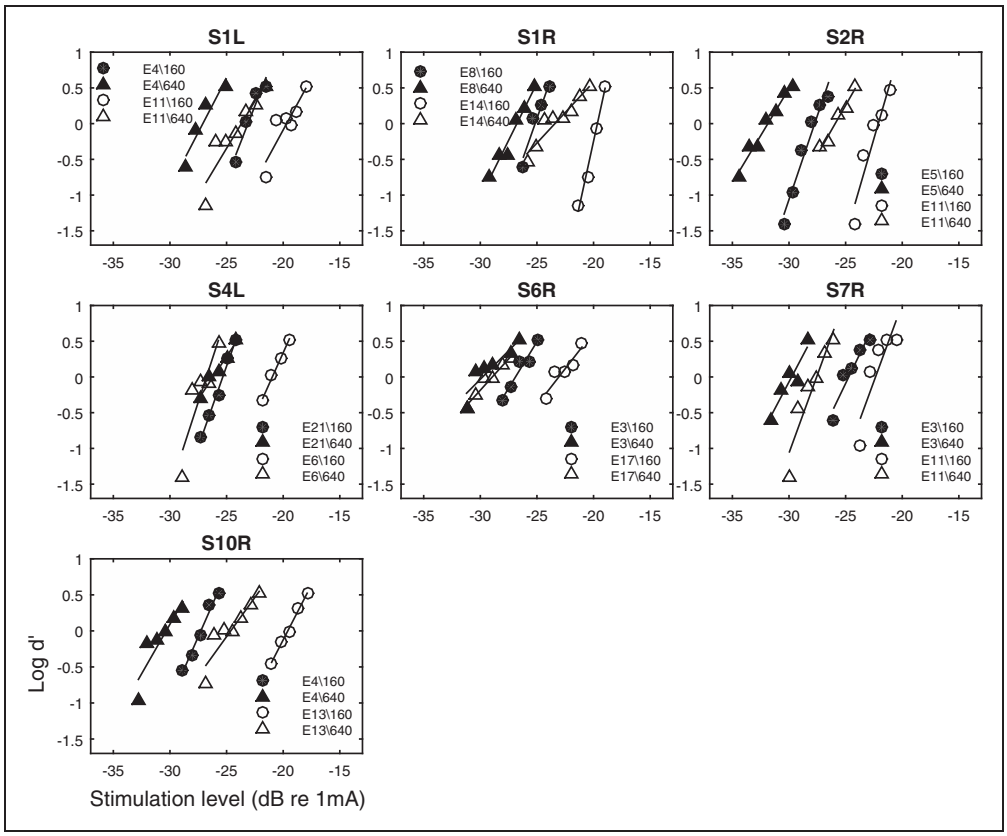

Figure 5. Psychometric functions for detection. Each panel shows data from one ear. The filled symbols show functions measured at one stimulation site for the 160 pps stimulus (circle) and the 640 pps stimulus (triangle). The open symbols show functions measured from the other stimulation site for the 160 pps stimulus (circle) and the 640 pps stimulus (triangle). The lines represent linear fit to the data.

and steepness of neural excitation growth with current level.

Loudness perceived with directly stimulating the auditory nerve bypasses the cochlear compressive nonlinearity and involves a frequency-dependent logarithmic transformation by the cochlear nucleus and an expansive nonlinearity performed by the brain (e.g., Zeng & Shannon, 1992; 1994). The practical loudness model assumes a direct link, although unproven, between loudness and the peripheral nerve output in the 3 to 7 ms temporal integration window (e.g., McKay, Henshall, Farrell, & McDermott, 2003; McKay & McDermott, 1998). That is, a given loudness, such as threshold, corresponds to a certain criterion number of neural spikes in the short integration window. A reduction in current required for achieving threshold as a result of an increase in stimulation rate depends on whether the increase in rate produces a corresponding increase in neural activity at a fixed current level. A greater ratio increase in neural activity with increasing stimulation rate results in a steeper threshold decrease. An increase in total neural activity can be achieved by either driving single fibers to respond at a higher discharge rate or engaging a larger neural population to respond to the stimulus.

Physiological studies in animals offered some insights into how single fibers might respond to an increase in stimulation rate at a fixed current level (e.g., Heffer et al., 2010). At the low and medium tested levels, electrically evoked single fiber response in acutely deafened guinea pigs appeared to be similar, if not less, as stimulation rate increased from 200 pps to 1000 pps. The suppression of neural excitability can be attributed to the fiber's refractory characteristics and accommodation to pulses that are below its threshold (Boulet, White, & Bruce, 2016). At a relatively high current level, each of the pulses in the 200 pps stimulus almost always evoked a spike, so did the onset of the 1000 pps stimulus, but the fiber quickly adapted to the rest of the stimulation, a phenomenon known as spike-rate adaptation (Hay-McCutcheon, Brown, & Abbas, 2005; Miller, Hu, Zhang, Robinson, & Abbas, 2008). The auditory fiber only responded to rate increase when the effect of partial depolarization (Cartee, van den Honert, Finley, & Miller, 2000; Middlebrooks, 2004) started to play a role as rate

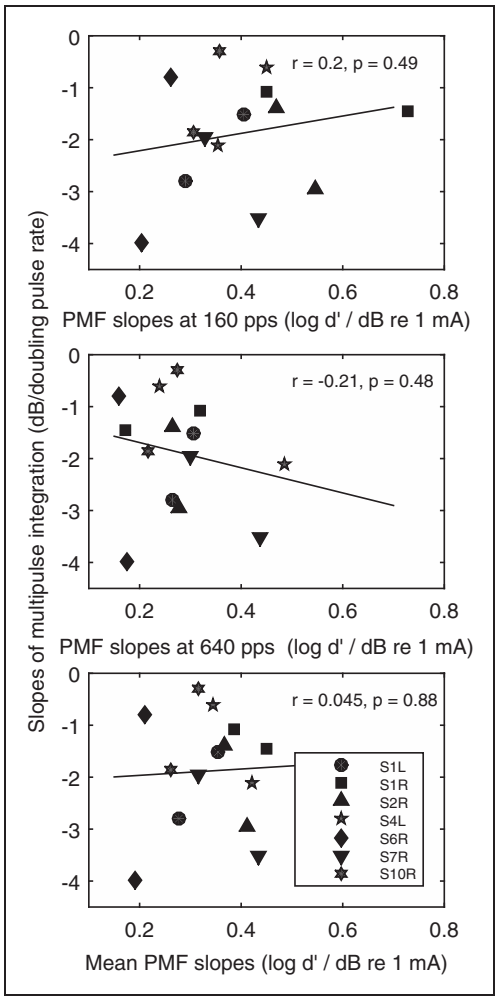

Figure 6. Scatter plot of the slopes of the multipulse integration functions against the slopes of the psychometric functions for detection for the 160 pps stimulus (top), the 640 pps stimulus (middle), and the averaged slopes for the two stimuli (bottom). Symbols represent ears (there are two data points per ear). Correlation coefficients and the *p* values are shown in the panels. The line represents linear fit to the data.

increased beyond 1000 pps. In the rate range that is relevant to the present study (<1000 pps), an increase in stimulation rate seems unable to drive single auditory fibers to produce a corresponding increase in neural activity over the course of the stimulus. The theory that MPI is dependent on the total number of excitable neurons is consistent with the observation in Zhou and Pfingst (2016b) and in the current study that broader psychophysical tuning at a high rate (900 pps) predicted steeper MPI (Figure 4). As rate increases, excitability of the activated neurons would be temporally constrained so they are unable to fire to each pulse in the pulse train. If the current field is broad, such as in the case of large electrode-neuron distance, and if we assume that the increase in stimulation rate would cause neurons at the edge of the current field to start responding because the neurons in the center of the current field are in an inhibited status, the total neural activity will increase with increasing stimulation rate. If the current field is narrow, the number of neurons that have not already been activated and thus are available to respond to stimulus is likely to be smaller than in the case of distant stimulation.

It is also likely that broad stimulation of the cochlea increases the probability of sampling and stimulating neurons that have good temporal sensitivity. The temporal response patterns can certainly vary considerably across fibers especially in chronically deafened auditory nerves (Hughes, Castioni, Goehring, & Baudhuin, 2012). Previous work has shown that monopolar electrodes resulted in more efficient charge integration (steeper thresholds vs. phase duration functions) as well as steeper electrically evoked compound action potential (ECAP) recovery functions than bipolar electrodes (Brown, Abbas, Borland, & Bertshy, 1996; Chatterjee & Kulkarni, 2014; Miller, Smith, & Pfingst, 1999; Smith & Finley, 1997). Moreover, shorter recovery constants of psychophysical forward masking predicted steeper MPI (Zhou & Pfingst, 2016a). These data suggest a possible link between MPI and the temporal sensitivity of the activated neurons. The relationship between MPI and SGN density in guinea pigs can then be understood in terms of SGN density covarying with neural health. That is, in guinea pigs with higher SGN density, the surviving neurons may also tend to be more responsive to stimulation, which has been reported in the literature (Zhou, Abbas, & Assouline, 1995).

Relationship Between MPI and PFD

The variation in MPI was further investigated in relation to the slope of the PFD. In both the hearing-impaired listeners and listeners with cochlear implants, reduced temporal integration, that is, shallow threshold versus duration functions, has been explained in terms of the abnormally steep *d'* versus stimulus level function (Carlyon, Buus, & Florentine, 1990; Donaldson, Viemeister, & Nelson, 1997). Presumably the slope of PFD reflects to a certain degree the composite neural input/output (I/O) function near the behavioral threshold. With cochlear implants, it has been proposed that in cochlear regions where there is sizable nerve loss, the current level must be elevated to achieve threshold, which might in turn excite the densely packed fibers in the internal auditory meatus, producing a steep neural excitation versus current level function. Such a steep neural excitation versus current level function, estimated by *d'* growth with current level, would predict a shallow MPI slope. The observation that higher SGN density as

well as lower absolute threshold level predicted steeper MPI in guinea pig studies is consistent with this idea (Kang et al., 2010; Pfingst et al., 2011; Zhou et al., 2015). However, results of the present study indicated that there is no relationship between the slope of the psychometric functions and the absolute threshold level, nor was there a relationship between the slope of the psychometric function and MPI. If the slope of PFD is related to loudness growth throughout the dynamic range, it would be predicted that a wider dynamic range or shallower loudness growth produces steeper MPI. However, this is contradictory to the literature that shows shallower loudness growth with the narrowing of current field (Bierer & Nye, 2014; Chatterjee, Fu, & Shannon, 2000; Chua, Bachman, & Zeng, 2011). Narrow stimulation in the current study (estimated by sharp tuning) was associated with shallow MPI. In summary, there does not seem to be evidence to suggest that, at least in MP stimulation, the steepness of PFD is related to the absolute threshold level, or related to MPI.

There was however a significant difference in the PFD slopes measured for the low-rate (160 pps) and high-rate (640 pps) stimuli (Figure 7), with the slopes for the 640 pps stimuli being significantly shallower than those for the 160 pps stimuli. It has been documented that neural noise increases with the increase of stimulation rate in single fibers such that their I/O functions flatten with rate, although the mechanism is poorly understood (White et al., 2012).

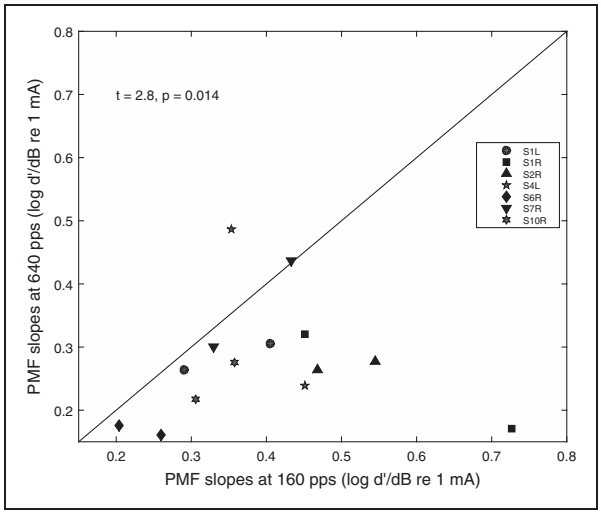

Figure 7. Scatter plot of the slopes of the psychometric functions for detection for the 640 pps stimulus against the slopes for the 160 pps stimulus. Stimulation sites and ears are collapsed in the plot. Symbols represent ears. Statistics for the *t* test comparing the slopes for the two stimuli are shown on the upper left corner of the plot.

Clinical Implications

Data in the present study showed that the low-rate thresholds were a better predictor for spatial tuning than high-rate thresholds, since a broad spatial activation might facilitate the detection of pulse trains that are of high rates resulting in low thresholds (Figure 2). This is consistent with our recent findings that showed a stimulus-dependent relationship between thresholds and the tuning measures (Zhou, 2016). Low-rate thresholds may be used as a quick clinical tool to identify channels that might interact with others at a rate relevant to what is typically used clinically in processor fittings (i.e., 900 pps/electrode). Methods such as current focusing or electrode removal may be used to reduce spectral smearing as a result of the interaction.

The finding that MPI is inversely related to spatial tuning reported here along with previous studies that investigated the effects of electrode configuration on charge integration and recovery (Brown et al., 1996; Chatterjee & Kulkarni, 2014; Smith & Finley, 1997; Miller et al., 1999) suggest that temporal sensitivity is often associated with broad activation of the cochlea. These results may imply the difficulty in achieving optimal temporal and spectral acuity at the same time in a degenerated auditory system. It remains to be tested how optimizing either the temporal or spectral resolution via customized mapping may affect the transmission of various temporally or spectrally dominant speech features.

Acknowledgments

The authors would like to thank the cochlear-implant subjects for their dedicated participation. The authors would also like to thank Mingqi Hang for assistance in data collection.

Declaration of Conflicting Interests

The authors declare no potential conflicts of interest regarding authorship or publication of this article.

Funding

The authors disclosed receipt of the following financial support for the research, authorship, and/or publication of this article: This work is supported by NIH NIDCD Grant R03 DC014771-01A1.

References

Bierer, J. A., & Nye, A. D. (2014). Comparisons between detection thresholds and loudness perception for individual cochlear implant channels. *Ear and Hearing*, *35*(6), 641–651.

Boulet, J., White, M., & Bruce, I. C. (2016). Temporal considerations for stimulating spiral ganglion neurons with cochlear implants. *The Journal of the Association for Research in Otolaryngology*, *17*(1), 1–17.

Brown, C. J., Abbas, P. J., Borland, J., & Bertschy, M. R. (1996). Electrically evoked whole nerve action potentials in Ineraid cochlear implant users: Responses to different stimulating electrode configurations and comparison to psychophysical responses. *Journal of Speech Hearing Research*, *39*(3), 453–467.

Carlyon, R. P., Buus, S., & Florentine, M. (1990). Temporal integration of trains of tone pulses by normal and by cochlearly impaired listeners. *The Journal of the Acoustical Society of America*, *87*(1), 260–268.

Cartee, L. A., van den Honert, C., Finley, C. C., & Miller, R. L. (2000). Evaluation of a model of the cochlear neural membrane. *I. Physiological measurement of membrane characteristics in response to intrameatal electrical stimulation*. Hearing Research, *146*(1-2), 143–152.

Chatterjee, M., Fu, Q. J., & Shannon, R. V. (2000). Effects of phase duration and electrode separation on loudness growth in cochlear implant listeners. *The Journal of the Acoustical Society of America*, *107*(3), 1637–1644.

Chatterjee, M., & Kulkarni, A. M. (2014). Sensitivity to pulse phase duration in cochlear implant listeners: Effects of stimulation mode. *The Journal of the Acoustical Society of America*, *136*(2), 829–840.

Chua, T. E. H., Bachman, M., & Zeng, F-G. (2011). Intensity coding in electric hearing: Effects of electrode configurations and stimulation waveforms. *Ear and Hearing*, *32*(6), 679–689.

Cosentino, S., Deeks, J., & Carlyon, R. P. (2015, July). *Spatial selectivity: How to measure and (maybe) improve it*. Paper presented at the Conference on Implantable Auditory Prostheses, Lake Tahoe, CA.

Donaldson, G. S., Viemeister, N. F., & Nelson, D. A. (1997). Psychometric functions and temporal integration in electric hearing. *The Journal of the Acoustical Society of America*, *101*(6), 3706–3721.

Eggermont, J. J. (1985). Peripheral auditory adaptation and fatigue: A model oriented review. *Hearing Research*, *18*(1), 57–71.

Hay-McCutcheon, J. M., Brown, J. C., & Abbas, J. P. (2005). An analysis of the impact of auditory-nerve adaptation on behavioral measures of temporal integration in cochlear implant recipients. *The Journal of the Acoustical Society of America*, *118*(4), 2444–2457.

Heffer, L. F., Sly, D. J., Fallon, J. B., White, M. W., Shepherd, R. K., & O'Leary, S. J. (2010). Examining the auditory nerve fiber response to high rate cochlear implant stimulation: Chronic sensorineural hearing loss and facilitation. *The Journal of Neurophysiology*, *104*(6), 3124–3135.

Hughes, M. L., Castioni, E. E., Goehring, J. L., & Baudhuin, J. L. (2012). Temporal response properties of the auditory nerve: Data from human cochlear-implant recipients. *Hearing Research*, *285*(1-2), 46–57.

Javel, E., & Shepherd, R. K. (2000). Electrical stimulation of the auditory nerve. *III. Response initiation sites and temporal fine structure*. Hearing Research, *140*(1-2), 45–76.

Javel, E., & Viemeister, N. F. (2000). Stochastic properties of cat auditory nerve responses to electric and acoustic stimuli and application to intensity discrimination. *The Journal of the Acoustical Society of America*, *107*(2), 908–921.

Kang, S. Y., Colesa, D. J., Swiderski, D. L., Su, G. L., Raphael, Y., & Pfingst, B. E. (2010). Effects of hearing preservation on psychophysical responses to cochlear implant stimulation. *The Journal of the Association for Research in Otolaryngology*, *11*(2), 245–265.

Kreft, H. A., Donaldson, G. S., & Nelson, D. A. (2004). Effects of pulse rate on threshold and dynamic range in Clarion cochlear-implant users (L). *The Journal of the Acoustical Society of America*, *115*(5), 1885–1888.

Long, C. J., Holden, T. A., McClelland, G. H., Parkinson, W. S., Shelton, C., Kelsall, D. C., . . . Smith, Z. M. (2014). Examining the electro-neural interface of cochlear implant users using psychophysics, CT scans, and speech understanding. *The Journal of the Association for Research in Otolaryngology*, *15*(2), 293–304.

Long, C. J., Melman, R. O., Parkinson, W. S., Holden, T. A., Potts, W. B., & Smith, Z. M. (2015, July). *Investigating the electro-neural interface: The effects of electrode position and age on neural responses*. Paper presented at the Conference on Implantable Auditory Prostheses, Lake Tahoe, CA.

Macmillan, N. A., & Creelman, C. D. (2005). *Detection theory: A user's guide*. Mahwah, NJ: Lawrence Erlbaum Associates.

McKay, C. M., Chandan, K., Akhoun, I., Siciliano, C., & Kluk, K. (2013). Can ECAP measures be used for totally objective programming of cochlear implants? *Journal of the Association for Research in Otolaryngology*, *14*(6), 879–890.

McKay, C. M., Henshall, K. R., Farrell, R. J., & McDermott, H. J. (2003). A practical method of predicting the loudness of complex electrical stimuli. *The Journal of the Acoustical Society of America*, *113*(4 Pt 1), 2054–2063.

McKay, C. M., & McDermott, H. J. (1998). Loudness perception with pulsatile electrical stimulation: The effect of interpulse intervals. *The Journal of the Acoustical Society of America*, *104*(2), 1061–1074.

Middlebrooks, J. C. (2004). Effects of cochlear-implant pulse rate and inter-channel timing on channel interactions and thresholds. *The Journal of the Acoustical Society of America*, *116*(1), 452–468.

Miller, C. A., Hu, N., Zhang, F., Robinson, B. K., & Abbas, P. J. (2008). Changes across time in the temporal responses of auditory nerve fibers stimulated by electric pulse trains. *Journal of the Association for Research in Otolaryngology*, *9*(1), 122–137.

Miller, A. L., Smith, D. W., & Pfingst, B. E. (1999). Across-species comparisons of psychophysical detection thresholds for electrical stimulation of the cochlea: II. Strength-duration functions for single, biphasic pulses. *Hearing Research*, *135*(1–2), 47–55.

Miller, C. A., Woo, J., Abbas, P. J., Hu, N., & Robinson, B. K. (2011). Neural masking by sub-threshold electric stimuli: Animal and computer model results. *Journal of the Association for Research in Otolaryngology*, *12*(2), 219–232.

Neff, D. L. (1986). Confusion effects with sinusoidal and narrow-band noise forward maskers. *The Journal of the Acoustical Society of America*, *79*(5), 1519–1529.

Parkins, C. W. (1989). Temporal response patterns of auditory nerve fibers to electrical stimulation in deafened squirrel monkeys. *Hearing Research*, *41*(2–3), 137–168.

Pfingst, B. E., Colesa, D. J., Hembrador, S., Kang, S. Y., Middlebrooks, J. C., Raphael, Y., . . . Su, G. L. (2011). Detection of pulse trains in the electrically stimulated

cochlea: Effects of cochlear health. *The Journal of the Acoustical Society of America*, *130*(6), 3954–3968.

Smith, R. L., & Brachman, M. L. (1982). Adaptation in auditory-nerve fibers: A revised model. *Biological Cybernetics*, *44*(2), 107–120.

Smith, D. W., & Finley, C. C. (1997). Effects of electrode configuration on psychophysical strength-duration functions for single biphasic electrical stimuli in cats. *The Journal of the Acoustical Society of America*, *102*(4), 2228–2237.

White, M., Heffer, L., Fallon, J., Sly, D., Shepherd, R., & O'Leary, S. (2012, February). *The slopes of auditory nerve input-output functions decrease as stimulus pulse rate is increased for spike-rates less than 100 spikes/second*. Paper presented at the Association for Research in Otolaryngology Midwinter Meeting, San Diego, CA.

Zeng, F.-G., & Shannon, R. V. (1992). Loudness balance between electric and acoustic stimulation. *Hearing Research*, *60*(2), 231–235.

Zeng, F.-G., & Shannon, R. V. (1994). Loudness-coding mechanisms inferred from electric stimulation of the human auditory system. *Science*, *264*(5158), 564–566.

Zhou, N. (2016). Monopolar detection thresholds predict spatial selectivity of neural excitation in cochlear implants: Implications for speech recognition. *PLoS One*, *11*(10), e0165476.

Zhou, R., Abbas, P. J., & Assouline, J. G. (1995). Electrically evoked auditory brainstem response in peripherally myelin-deficient mice. *Hearing Research*, *88*(1–2), 98–106.

Zhou, N., Kraft, C. T., Colesa, D. J., & Pfingst, B. E. (2015). Integration of pulse trains in humans and guinea pigs with cochlear implants. *The Journal of the Association for Research in Otolaryngology*, *16*(4), 523–534.

Zhou, N., & Pfingst, B. E. (2016a). Evaluating multipulse integration as a neural-health correlate in human cochlear-implant users: Relationship to forward-masking recovery. *Journal of the Acoustical Society of America*, *139*(3), EL70–75.

Zhou, N., & Pfingst, B. E. (2016b). Evaluating multipulse integration as a neural-health correlate in human cochlear-implant users: Relationship to spatial selectivity. *The Journal of the Acoustical Society of America*, *140*, 1537–1547.

Zhou, N., & Pfingst, B. E. (2014). Relationship between multipulse integration and speech recognition with cochlear implants. *The Journal of the Acoustical Society of America*, *136*(3), 1257–1268.

Zhou, N., Xu, L., & Pfingst, B. E. (2012). Characteristics of detection thresholds and maximum comfortable loudness levels as a function of pulse rate in human cochlear implant users. *Hearing Research*, *284*(1–2), 25–32.